

CONCLUSIONS OF THE WORKSHOP ON THE INTERFEROMETRIC MODE OF OSIRIS

Margarita Rosado¹

RESUMEN

Se presentan las conclusiones del taller realizado para definir los programas científicos y, en consecuencia, las características de interferómetros de Fabry-Perot de barrido de altos órdenes propuestos para ser acoplados al instrumento OSIRIS del GTC.

ABSTRACT

We present the conclusions of the workshop organized to define the scientific drivers and the derived main characteristics of high-order scanning Fabry-Perot interferometers proposed to be coupled to OSIRIS at the GTC.

Key Words: INSTRUMENTATION: SPECTROGRAPHS — GALAXIES: KINEMATICS AND DYNAMICS — GALAXIES: INTERACTIONS — COSMOLOGY: DARK MATTER — ISM: KINEMATICS AND DYNAMICS

1. INTRODUCTION

After the “II International Workshop on Science with the GTC: Science with GTC 1st-light Instruments and the LMT”, several attendants participated in a workshop aimed at analyzing the scientific drivers and logistics of the interferometric mode of the OSIRIS instrument conceived to work with the Gran Telescopio de Canarias (GTC).

In this workshop we have reviewed several scientific projects that could be done advantageously with high-order scanning Fabry-Perot (FP) interferometers in OSIRIS. The subjects of these projects have a wide scope: from star formation and interstellar matter in our Galaxy to extragalactic astronomy. The speakers were: Jordi Cepa, Jesús González, Eduardo de la Fuente, Alejandro Raga, Pablo Velázquez, Erika Benítez, José A. de Diego, Margarita Valdez, Ivanio Puerari, Patricia Ambrocio, Lorena Arias, Alfredo Franco, John Beckman, Carlos Gutiérrez, Abel Bernal and Margarita Rosado.

In what follows, a presentation of the main ideas and motivations of some of the projects is given. The conclusions and planning strategies are given at the end.

2. DETECTION AND KINEMATICS OF PROTOPLANETARY DISKS AROUND YOUNG STARS (EDUARDO DE LA FUENTE)

The interferometric mode of the OSIRIS spectrograph of the GTC could give highly accurate, kinematical information of protoplanetary disks (proplyds); photoevaporating circumstellar disks around young stellar objects. Using the scanning Fabry-Perot interferometer “PUMA” (Rosado, Langarica, Bernal et al. 1995) with the 2.1 meter telescope at OAN-SPM, de la Fuente, Rosado, Arias, et al. (2003) obtained radial velocity profiles of 13 proplyds and 3 proplyd candidates, determining their radial velocities, mass loss rates and disk lifetimes. Several of them present monopolar microjets. These authors found the Fabry-Perot technique to be an effective method of detecting and identifying proplyds in the Orion Nebula because they can be detected as clearly point-like nebular objects. This is seen in the raw Fabry-Perot data cubes (see Rosado, de la Fuente, Arias, Rosado, Salas & Cruz-Gonzalez 2001) where the contamination of the bright HII region is severe and more clearly, in the unsharp-masked and HII region subtracted (see Figure 1) data cubes. There is evidence that the [OI](λ 6300Å) ion is a good tracer of the photoevaporated flow initial velocity (V_o) because this line seems to be associated with the flow of neutral gas, so it is necessary to make studies and observations in this line, given that V_o is a very important parameter for obtaining the mass loss rate. Furthermore, Fabry-Perot studies in lines

¹Instituto de Astronomía, UNAM, México.

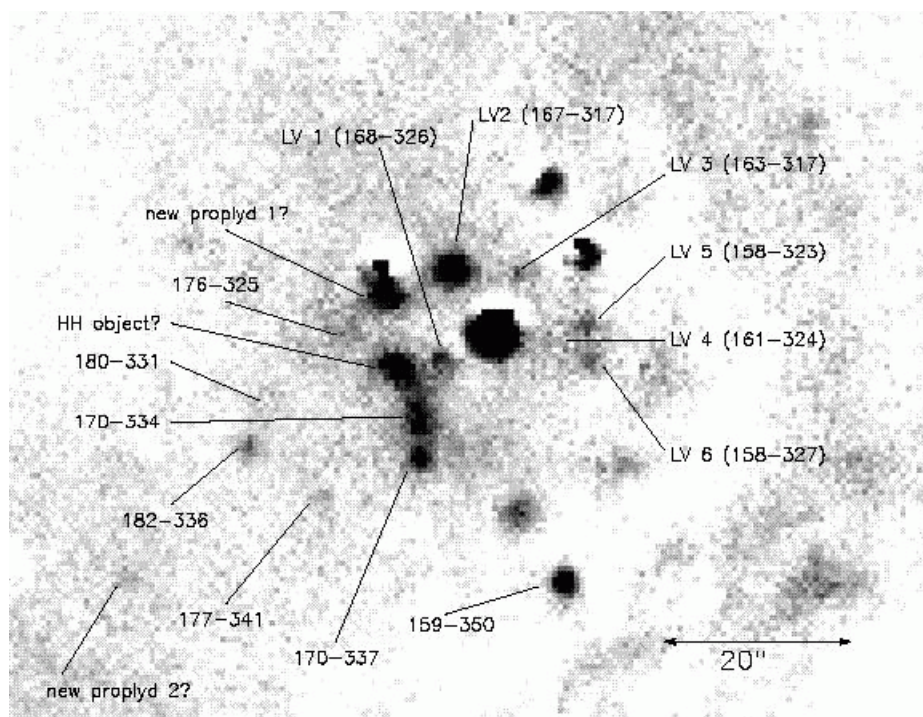


Fig. 1. HII region-subtracted $H\alpha$ velocity map at the heliocentric velocity of $+119 \text{ km s}^{-1}$ of the central part of the Huygens Region (de la Fuente et al. 2003). The identified proplyds are marked. The brightest point at the center is Θ^1 C Orionis. North to the top. East to the left.

such as $H\alpha$, [NII], [SII] and [OIII], among others, of proplyds in the Orion Nebula are scarce. So, it is very important to obtain 3D spectrometry in all these lines, compare the data obtained with different kinds of 3D spectrographs, in order to obtain and understand the kinematics of these objects and, thus to contribute to the knowledge of their nature.

3. INSTALLING, OPERATING AND REMOTIZING THE SCANNING FABRY-PEROT INTERFEROMETERS IN THE INSTRUMENTS PUMA AND PUMILA (ABEL BERNAL & LUIS ARTEMIO MARTÍNEZ)

We have developed two instruments which use scanning Fabry-Perot (FP) interferometers in order to obtain the radial velocity profiles at every point within the whole extent of a nebula or galaxy. To study the molecular gas we are developing PUMILA, which use a scanning FP interferometer optimized in the near IR (see Rosado et al. 1999 and Arias et al. 2001). It has been used to obtain velocity-cubes of the line at $2.12\mu\text{m}$ of the molecular hydrogen, corresponding to the $v = 1-0$ rotational transition. To study the emission lines of the ionized gas

we have developed the UNAM scanning FP interferometer PUMA (Rosado et al. 1995), optimized in the red, which allows to obtain velocity-cubes at $H\alpha$, [NII] λ 6583 Å [SII] λ 6717 and 6731 Å and [OIII] λ 5007 Å. The sampling spectral resolutions of the FP interferometers are about: 10 and 20 km s^{-1} for the IR and visible, respectively. The experience acquired in the developing of these instruments could be used in the characterization of high-order Fabry-Perot interferometers coupled to OSIRIS.

PUMA is an integral field spectrometer having as the dispersive element a scanning Fabry-Perot interferometer. It works at optical wavelengths. PUMILA (PUMA-CAMILA) is a prototype instrument consisting of a scanning Fabry-Perot interferometer optimized in the near infrared, inserted in the CAMILA IR camera. Both instruments are attached to the 2.1m telescope of the Observatorio Astronómico Nacional at San Pedro Mártir, B.C. México (OAN).

The PUMA is fully automatized allowing the electronic control of its movable parts as well as the separation and parallelism of the FP. PUMA's mechanical structure is made of aluminium with a flex-

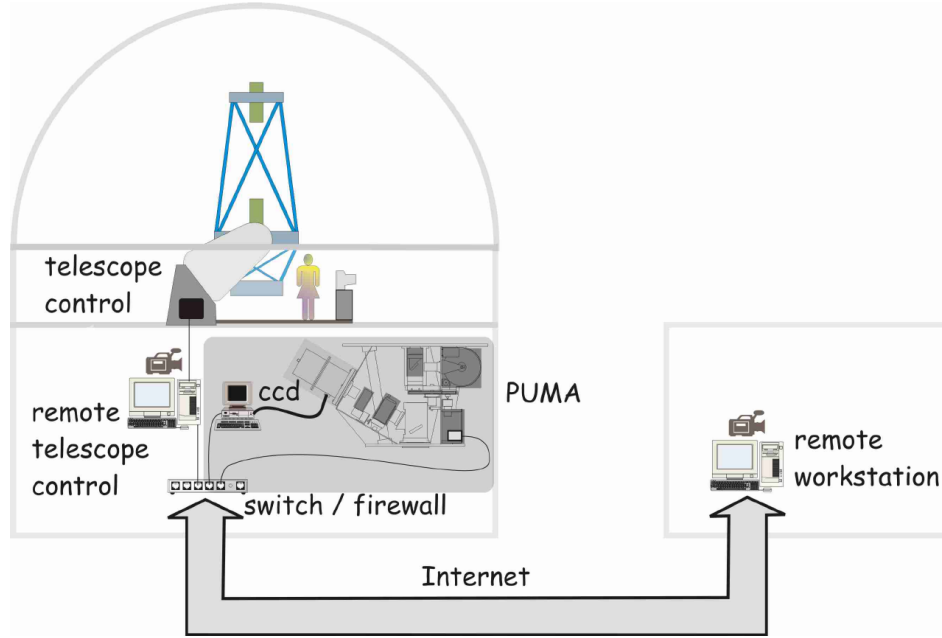


Fig. 2. PUMA setup and remote control system.

ure tolerance of $10\ \mu\text{m}$, i.e., half the detector's pixel size. Its movable parts are: two field diaphragms, a filter wheel with 8 positions, the calibration system, a mechanism that allows the displacement of the FP and a 4-prism arm used to settle the FP parallelism. The instrument is operated remotely via internet using a PC-Linux workstation. Figure 2 shows the proposed PUMA setup at the OAN conceived for remote observations.

PUMA characteristics:

Focal reducer 2:1 (from $f/7.9$ to $f/3.95$); field of view: $10'$; spectral range: from 3650 to $8650\ \text{\AA}$; plate scale: $0.67'' \times px^{-1}$; detector: 1024×1024 thinned CCD of $24\mu\text{m}$ pixel size; interference filters: $H\alpha$, [NII], [SII] and [OIII]; calibration lamps: hydrogen, helium and neon. Fabry-Perot: Queensgate ET-50, $Finesse = 24$; interference order: 330; free spectral range: $19.8\ \text{\AA}$; spectral resolution: $0.414\ \text{\AA}$, at $H\alpha$.

PUMILA characteristics:

Field of view: $3'.67 \times 3'.67$; spectral range: from 1.4 to $2.5\ \mu\text{m}$; plate scale: $0.86'' \times px^{-1}$; detector: 256×256 NICMOS3; interference filters: $Br\gamma$, H_2 , CO. Fabry-Perot: Queensgate ET-50WF, $Finesse = 16$; free spectral range: $624\ \text{km s}^{-1}$; velocity resolution: $10\ \text{km s}^{-1}$, at $1.5\ \mu\text{m}$.

4. KINEMATICS OF HERBIG-HARO OBJECTS (ALEJANDRO RAGA)

We have obtained an $H\alpha$ position-velocity cube from Fabry-Perot interferometric observations of the

HH 110 flow. We analyze the results in terms of anisotropic wavelet transforms, from which we derive the spatial distribution of the knots, as well as their characteristic sizes (along and across the out-flow axis). We then study the spatial behavior of the line width and the central radial velocity. The results are interpreted in terms of a simple "mean flow plus turbulent eddy" jet/wake model. We find that most of the observed kinematics appears to be a direct result of the mean flow, on which are superposed low-amplitude ($\sim 35\ \text{km s}^{-1}$) turbulent velocities. Further details could be found in Beck, Riera, Raga & Aspin (2003).

5. SHOCKS IN THE MOLECULAR ENVELOPES OF BIPOLAR PLANETARY NEBULAE (LORENA ARIAS)

The study of the interplay between ionized and molecular gas in planetary nebulae (PNe) can be approached by analyzing the kinematics of the line at $2.12\mu\text{m}$ of the H_2 , for the molecular gas, and of the lines of $H\alpha$, [NII], [SII] and [OIII], for the ionized gas.

According to theoretical models, bipolar PNe are the result of a non-uniform distribution of material ejected by the central star while it passes through the AGB phase. Consequently, the study of the kinematics of ionized and molecular gas in PNe could give important insights on how the ejection is accomplished,

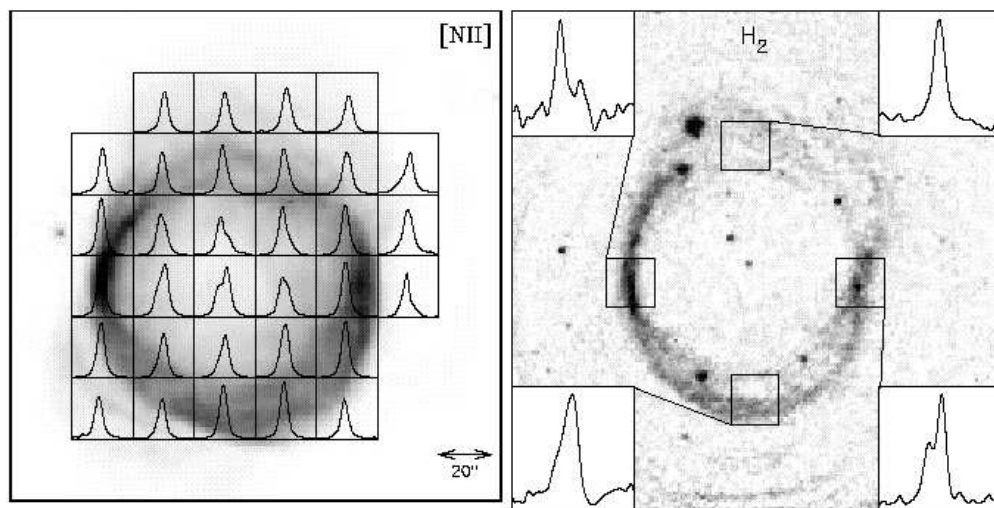


Fig. 3. Fabry-Perot velocity maps of the PN NGC 6781 corresponding to the emission of [NII] at -66 km s^{-1} (left panel) and the $2.12 \mu\text{m}$ H₂ line at -46 km s^{-1} (right panel). Integrated radial velocity profiles of different zones are shown superimposed.

on the amount of ejected gas and timescales. The observations of the interplay between ionized and molecular gas in PNe could serve to know whether the “colliding winds” model proposed by Kwok, Purton & FitzGerald (1978) describes the reality or not.

Here we only discuss the case of the PN NGC 6781. This PN has been classified as elliptical because of its ring-shaped morphology. However, our kinematical analysis allows us to show that the true shape of NGC 6781 is bipolar, having the pole axis seen almost perpendicular to the plane of the sky.

We have obtained direct images in the lines of H α , [NII], [SII] and [OIII] for the ionized gas, as well as in the lines of H₂ at $2.12 \mu\text{m}$ and $2.24 \mu\text{m}$ for the molecular gas. We show that the ratio between the lines S(1) 2-1 (at $2.24 \mu\text{m}$) and S(1) 1-0 (at $2.12 \mu\text{m}$) is much smaller than 0.5, implying shock excitation. In addition, we have obtained flux-calibrated FP velocity-cubes in the lines of H α and [NII] and in the line of H₂ at $2.12 \mu\text{m}$ for studying the ionized and molecular gas kinematics, respectively. These data were obtained using the visual-light optimized PUMA (Rosado et al. 1995) and near IR-light optimized PUMILA (Rosado et al. 1999) instruments at the 2.1m telescope of the OAN. These Fabry-Perot data allow us to show that the kinematics of the molecular gas is quite similar to the kinematics of the ionized gas. Furthermore, we obtain splitting of the velocity profiles at the center of the ring indicating that the true morphology of this object is bipolar having its poles in the direction of the line of

sight. We also could measure the shock velocities of the H₂ and propose a geometrical model for the H₂ emission.

In Figure 3 (from Arias & Rosado 2002) we show typical radial velocity profiles of the [NII] ($\lambda 6584 \text{ \AA}$) and the H₂ emission line at $2.12 \mu\text{m}$, superimposed on the Fabry-Perot velocity maps of NGC 6781 corresponding to the emissions of [NII] at -66 km s^{-1} and H₂ at -46 km s^{-1} , respectively. Since our FP velocity cubes allow us to obtain radial velocity profiles of each pixel over the whole extension of this PN, we are able to obtain position-velocity diagrams that could be used to fit a geometrical model. The selected geometrical model that best fit the observed position-velocity diagrams is the one consisting of two thin ellipsoidal closed shells with a velocity law increasing with distance from the PN nucleus. We were able to derive the inclination angle of the pole axis relative to the plane of the sky (75°) and the expansion velocity at the torus (13 km s^{-1}). Since the expansion velocities are supersonic, we have shown, by kinematic means, that shocks are exciting the molecular hydrogen. We also obtain an estimate of $0.2 M_\odot$ for the mass of the unshocked H₂ in the PN while the mass of the ionized gas amounts to $0.13 M_\odot$. This is an independent way of estimating the mass of gaseous PNe envelopes.

6. DYNAMICS OF BARRED GALAXIES (JOHN BECKMAN)

We present emission line mapping of the strongly barred galaxy NGC 1530 obtained using Fabry-Perot

interferometry in $H\alpha$, at significantly enhanced angular resolution compared with previously published studies (Zurita, Relaño, Beckman & Knapen 2004). The observations were carried out using TAURUS instrument attached to the WHT at La Palma. The main point of the work is to examine in detail the non-circular components of the velocity field of the gas, presumably induced by the strongly non-axisymmetric gravitational potential of the bar. To do this we first derive a model rotation curve making minimum assumptions about kinematic symmetry, and go on to measure the non-circular component of the full radial velocity field. This clearly reveals the streaming motions associated with the spiral density wave producing the arms, and the quasi-elliptical motions with speeds of order 100 km s^{-1} aligned with the bar. It also shows in some detail how these flows swing in towards and around the nucleus as they cross a circumnuclear resonance, from the dominant “x1 orbits” outside the resonance to “x2 orbits” within it. Comparing cross-sections of this residual velocity map along and across the bar with the surface brightness map in $H\alpha$ indicates a systematic offset between regions of high non-circular velocity and massive star formation. To investigate further we produce maps of velocity gradient along and across the bar. These illustrate very nicely the shear compression of the gas, revealed by the location of the dust lanes along loci of maximum velocity gradient perpendicular to the bar. They also show clearly how shear, seen in our data as velocity gradient perpendicular to the flow, acts to inhibit massive star formation, whereas shocks, seen as strong velocity gradients along the flow vector, act to enhance it. Although the inhibiting effect of gas shear flow on star formation has long been predicted, this is the clearest observational illustration so far of the effect, thanks to the strong shock-induced counterflow system in the bar. It is also the clearest evidence that dust picks out shock-induced inflow along bars. These observations should be of considerable interest to those modelling massive star formation in general.

7. DYNAMICS OF IRREGULAR GALAXIES (MARGARITA VALDEZ-GUTIÉRREZ)

Fabry-Perot interferometers are the ideal instruments to study the kinematics of the ionized gas in irregular galaxies in both global and local scales. As an example, the results obtained for the irregular galaxy NGC 4449 are presented.

A detailed kinematic analysis of ionized gas in the nearby irregular galaxy NGC 4449 was done by means of Fabry-Perot interferometry using the spec-

tral lines of $H\alpha$ and [S II] (Valdez-Gutiérrez, Rosado, Puerari et al. 2002) with the PUMA instrument at the 2.1m telescope at OAN. We have analyzed the global velocity field, the spatially extended diffuse gaseous component, and the H II region populations and, furthermore, have determined the rotation curve based on the heliocentric radial velocities of the global $H\alpha$ spatial distribution. Our results for NGC 4449 show that the optical velocity field decreases in radial velocity along the optical bar from northeast to southwest, presenting an anti-correlation relative to the outer velocity field of the H I component. This is in agreement with previous studies. The diffuse gaseous component (DIG) that permeates the entire galaxy is analyzed in terms of its radial velocity field, as well as its velocity dispersions. We find that the DIG component presents peculiar kinematic features, such as abrupt velocity gradients and highly supersonic velocity dispersions ($\sigma \sim 4$ times the values of the nearest H II regions), but that its kinematic and dynamical influence is important on both global and local scales. The optical rotation curve of this nearby irregular galaxy shows that the northeast sector rotates like a solid body ($V_{ROT} = 40 \text{ km s}^{-1}$ at $R = 2 \text{ kpc}$). In contrast, for the southwest side our results are not conclusive; the behavior of the gas at those locations is chaotic. We conclude that the origin of such complex kinematics and dynamics is undoubtedly related to the aftermath of an interaction experienced by this galaxy in the past.

8. DYNAMICS OF ISOLATED PAIRS OF GALAXIES (MARGARITA ROSADO)

Pairs of galaxies which are isolated from other galaxies are the simplest cases of interaction between galaxies. The degree of interaction between the members of the pair appears to be variable: from a first, fly-by encounter, where the galaxies never lose their identity, to a merger, where the galaxies fusion. Usually, numerical simulations are confronted only with the morphological signs of the encounter: tidal tails, common envelopes of stars and gas, bridges and so on. However, it is also important to confront the velocity fields of the galaxy pairs with models.

Obtaining the kinematics of isolated galaxy pairs requires the use of Fabry-Perot interferometers because of the asymmetries developed in the galaxies during the encounter. In that way, it is possible to obtain the 2D radial velocity field, velocity dispersions and residual velocities at each pixel of the field of view. We present $H\alpha$ observations of the isolated interacting galaxy pair NGC 5426/27

(Arp 271) using the scanning Fabry-Perot interferometer PUMA (Fuentes-Carrera, Rosado, Amram et al. 2004). Using the FP data, the velocity field, various kinematical parameters and rotation curve for each galaxy were derived. The FWHM map and the residual velocities map were also computed to study the role of non-circular motions of the gas. Most of these motions can be associated with the presence of spiral arms and structures such as central bars. We found a small bar-like structure in NGC 5426, a distorted velocity field for NGC 5427 and a bridge-like feature between both galaxies which seems to be associated with NGC 5426. Using the observed rotation curves, a range of possible masses was computed for each galaxy. These were compared with the orbital mass of the pair derived from the relative motion of the participants. The rotation curve of each galaxy was also used to fit different mass distribution models considering the most common theoretical dark halo models.

Fabry-Perot interferometers are also required to explore the dark matter distribution of galaxies. Fuentes-Carrera, Amram & Rosado (2002) studied the interacting galaxy pair NGC 3893/96 (Kar 302), an M51-type galaxy pair, by means of FP interferometry. In this particular case, the derived velocity field and rotation curve of the main galaxy (NGC 3893) allows us to show that the galaxy follows a rather axisymmetric behavior. Together with HI observations, several mass models were adjusted in order to study the nature of the dark halo as well as the mass-to-light ratio of the galaxy. We find that in order to constrain these models, it is important to have a high resolution H α rotation curve for the inner parts of the galaxy.

9. DISCUSSION AND CONCLUSIONS

9.1. Advantages of scanning Fabry-Perot interferometers with respect to IFUs and MOSs

9.1.1. Integral Field Units (IFUs)

Scanning Fabry-Perot interferometers also are integral field spectrometers; however, this name is nowadays given to instruments that divide the image of an extended object into small zones by means of microlenses or optical fiber arrays. In this way, it is possible to obtain simultaneous spectra over the different zones by means of grisms and dispersion gratings. Usually, IFUs provide a small field of view ($\sim 10''$) and relatively low spectral resolutions ($R \sim 2000$ to 5000). A FP in OSIRIS will obtain high spectral resolution data (up to $R = 20000$) over the whole OSIRIS' field of view ($8'$).

9.1.2. Multi-object spectrometers (MOSs)

This kind of instruments are optimum when it is required to get low spectral resolution spectra ($R \sim 2000$ to 5000) of a collection of point-like objects, well separated within them, and distributed over a large field (i.e., $\sim 10'$). However, MOSs are less useful (1) when the object under study is extended and asymmetric, (2) when the different objects are not point-like but extended and spectra of different regions within an object are required or, (3) when higher spectral resolution is wanted. In those cases, a FP is more advantageous because it will provide high spectral resolution spectra over all the spatial elements (pixels) of a field.

9.2. Logistics and required FP characteristics

Required FPs will be installed within the OSIRIS' collimated beam in the filter wheel hosting the tunnable filters (TFs). In addition, the FP interferometric mode of OSIRIS requires the use of a set of current interferometric filters (fixed gap, low-order FPs) that act as band-pass filters isolating the desired line. These filters will be installed in the second filter wheel of OSIRIS, also within the collimated beam. The same controller used for the TFs (a CS100 controller) could be used to control the FP separation. Calibrations could be done using lamps of H, He, Ne and Ar.

The required etalons are ICOS ET100 and, according to the projects presented at this workshops, it would be convenient to acquire at least two of them, optimized in the spectral ranges from 6300 to 7000 Å (Galactic projects and redshifted Lyman α emitters) and from 8000 to 9500 Å (OTELLO objects kinematics), respectively. Moreover, they could have two different spectral resolution:

- High resolution etalon: with $R = 20000$ (velocity resolution of 15 km s^{-1} and free spectral range of 600 km s^{-1}) and
- Low resolution etalon: with $R = 5000$ (velocity resolution of 60 km s^{-1} and free spectral range of 1000 km s^{-1}).

9.3. Financial support

– From Mexico: Margarita Rosado has submitted a proposal to CONACYT in order to get funds for one FP etalon and 7 interference filters. The project is being refereed.

– From Spain: Jordi Cepa thinks that it is possible to get some funds from the 'Fondos para infraestructura y mejoras' if the acquisition of etalons and filters are proposed as improvements to OSIRIS.

– From the CEE: Jordi Cepa informed that since Spain is not member of ESO, it is difficult to get

funds from the CEE to GTC instruments. However, the situation could change when Spain would become a member of ESO.

9.4. *Comparison with similar instruments in large telescopes*

There are operating only two similar instruments in large telescopes:

- KYOTO 3D at the SUBARU telescope; with a field of view $\leq 2'$

and

- PFIS at the SALT telescope; with a field of view $\leq 3'$

Consequently, a FP in OSIRIS, with a field of view $\leq 8'$ would be competitive and high performance instrument for the next years to come. It would be an unique instrument for a variety of problems requiring a large field of view.

9.5. *Use policies in the GTC*

Two possible use policies have been analyzed:

- a) That the FP is considered as a VISITING instrument

or

- b) That the FP is considered as a PRIVATE instrument

In the case of a VISITING instrument, it would be possible to get guaranteed time. However, the FP working group would supply manuals and data reduction software. In this case, the instrument should be used by the whole community.

In the case of a PRIVATE instrument, it is not necessary to write manuals nor to supply the data reduction software; each observer would manage to use his preferred data reduction software. In this case, there would not be guaranteed time and the group responsible of the FP would use the normal means to get observing time at the GTC.

As a start, it has been considered that the FP mode of OSIRIS could start as a PRIVATE instrument and, if it is requested by an important number of observers, then, to change the status to VISITING instrument. In this case, it would be worth to elaborate manuals and data reduction software compatible with GTC standards.

The group responsible of the FP is constituted of the astronomers signing the successful fund proposals.

MR wishes to thank the attendants to this nice and collaborative workshop. She also wishes to acknowledge the financial support from grants IN120802 of DGAPA-UNAM and 2002-C01-40095 of CONACYT.

REFERENCES

- Arias, L., & Rosado, M. 2002, RevMexAA Ser. Conf., 12, 138
- de la Fuente, E., Rosado, M., Arias, L., & Ambrocio-Cruz, P. 2003, RevMexAA, 39, 127
- Fuentes-Carrera, I., Amram, P., & Rosado, M., 2002, Ap&SS, 281, 411
- Fuentes-Carrera, I., Rosado, M., Amram, P., et al. 2004, A&A, 415, 451
- Kwok, S., Purton, C. R., & FitzGerald, P.M. 1978, ApJ, 219, L125
- Beck, T. L., Riera, A., Raga, A. C., & Aspin, C. 2003, AJ, 127, 408
- Rosado, M., Langarica, R., Bernal, A., Cobos, F., et al. 1995, RevMxAA Ser. Conf., 3, 268
- Rosado, M., et al. 1999, Proc. SPIE, 3354, 1111
- Rosado, M., de la Fuente, E., Arias, L., Raga, A., & Le Coarer E. 2001, AJ, 122, 1928
- Valdez-Gutiérrez, M., Rosado, M., Puerari, I., et al. 2002, AJ, 124, 3157
- Zurita, A., Relaño, M., Beckman, J., & Knapen, J. H. 2004, A&A, 413, 73